REPORT DOCUMENTATION PAGE

AFRL-SR-AR-TR-09-0217

PLEASE DO NOT RETURN YOUR FORM TO THE ABOVE ADDRESS.

1. REPORT DATE *(DD-MM-YYYY)*	2. REPORT TYPE	3. DATES COVERED (From – To)
	Final Technical Report	1 JAN 2007 – 31 MAY 2008

4. TITLE AND SUBTITLE
HIGH-FIDELITY REAL GAS MODEL FOR RF EXCITED PLASMA FLOW CONTROL

5a. CONTRACT NUMBER

5b. GRANT NUMBER
FA9550-07-1-0131

5c. PROGRAM ELEMENT NUMBER

6. AUTHOR(S)
SUBRATA ROY

5d. PROJECT NUMBER

5e. TASK NUMBER

5f. WORK UNIT NUMBER

7. PERFORMING ORGANIZATION NAME(S) AND ADDRESS(ES)
336 MAE-B
PO BOX 116250
GAINESVILLE, FL 32611-6250

8. PERFORMING ORGANIZATION REPORT NUMBER

9. SPONSORING/MONITORING AGENCY NAME(S) AND ADDRESS(ES)
USAF/AFRL
AFOSR
875 North Randolph Street
Arlington VA 22203

10. SPONSOR/MONITOR'S ACRONYM(S)
AFOSR

11. SPONSORING/MONITORING AGENCY REPORT NUMBER
N/A

12. DISTRIBUTION AVAILABILITY STATEMENT

Distribution Statement A: Approved for public release. Distribution is unlimited.

13. SUPPLEMENTARY NOTES

14. ABSTRACT

This report is a summary of a one-year effort on modeling air plasma actuators by the PI¿s research team and collaborators. Plasma actuators have become the key enabler for boundary layer flow control especially when the device needs to be surface compliant. While the effects of these actuators are striking for low speeds, their efficacy becomes very limited for a wide range of flow speeds due to the lack of understanding of the multiphysics controlling adjustable authority of such devices. In our previous effort we have demonstrated the prediction capability of module-based multiscale ionized gas (MIG) flow finite-element code for mitigating inert gas flow separation using rf-driven dielectric barrier discharge. In this effort we: (1) develop multi-dimensional first principles based N2/O2 air chemistry models for the non-equilibrium real gas discharge, and (2) implement it in a finite element framework to predict plasma discharge characteristics and its associated electric force generation over a three-dimensional conical forebody geometry. To our knowledge, such detailed plasma kinetics based effort has not been reported before. During the development of this project we have worked in close collaboration with RBAC/AFRL researchers to integrate MIG results with FDL3DI code and to simulate electrodynamic mitigation over practical surface.

15. SUBJECT TERMS

16. SECURITY CLASSIFICATION OF:			17. LIMITATION OF ABSTRACT	18. NUMBER OF PAGES	19a. NAME OF RESPONSIBLE PERSON
a. REPORT	b. ABSTRACT	c. THIS PAGE	Unclassified	21	19b. TELEPONE NUMBER (*Include area code*)

07-NA-108

FINAL REPORT FOR AFOSR GRANT NUMBER FA9550-07-1-0131

PROJECT TITLE: HIGH-FIDELITY REAL GAS MODEL FOR RF EXCITED PLASMA FLOW CONTROL - A Three Dimensional Analysis with Air Chemistry

Principal Investigator: Subrata Roy
Department of Mechanical and Aerospace Engineering
University of Florida
Gainesville, FL 32611

Abstract

This report is a summary of a one-year effort on modeling air plasma actuators by the PI's research team and collaborators. Plasma actuators have become the key enabler for boundary layer flow control especially when the device needs to be surface compliant. While the effects of these actuators are striking for low speeds, their efficacy becomes very limited for a wide range of flow speeds due to the lack of understanding of the multiphysics controlling adjustable authority of such devices. In our previous effort we have demonstrated the prediction capability of module-based multiscale ionized gas (MIG) flow finite-element code for mitigating inert gas flow separation using rf-driven dielectric barrier discharge. In this effort we: (1) develop multi-dimensional first principles based N_2/O_2 air chemistry models for the non-equilibrium real gas discharge, and (2) implement it in a finite element framework to predict plasma discharge characteristics and its associated electric force generation over a three-dimensional conical forebody geometry. To our knowledge, such detailed plasma kinetics based effort has not been reported before. During the development of this project we have worked in close collaboration with RBAC/AFRL researchers to integrate MIG results with FDL3D1 code and to simulate electrodynamic mitigation over practical surface.

I. INTRODUCTION

The experiments and numerical predictions [1-9] reported lately show the ability of plasma actuators to impart body force inside the boundary layer of a fluid in the close vicinity of a surface. For plasma actuators with spatially displaced electrodes the airflow inducement is close to the dielectric surface with a time-averaged flow velocity measured between 1-3 m/s. These actuators exhibit several benefits in active flow control applications, including absence of moving parts, rapid on-off deployment and attractive self-limiting characteristics. Figure 1 represents a standard two-dimensional geometry which has been extensively investigated for boundary layer flow control at low speeds. The asymmetric positioning of the electrodes helps directional bias of the majority electric force and hence inducement of a wall jet. The induced force is local (within a few mm) and dissipates rapidly outside the domain of influence.

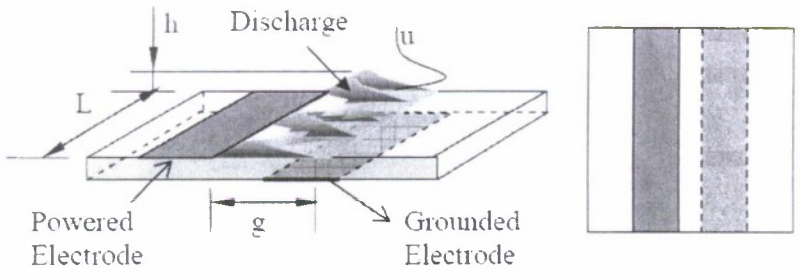

Figure 1. Standard linear plasma actuator with primarily two-dimensional discharge and induced velocity.

The discharge may be characterized as transient with a time scale of the order of a few microseconds while that for the bulk gas flow is in milliseconds. This allows the fluid to respond relatively instantaneously to the electrical inputs. Such force successfully controls flow separation on airfoils at a high angle-of-attack, increases the lift and/or reduces the drag of airfoils and fuselages. Despite experimental success, applications of such actuators are limited to low speeds due to an incomplete understanding of the plasma-gas coupling in all scales and dimensions. For example, to our knowledge, the reported numerical efforts are either one or two-dimensional, and the

experimental efforts lack temporal and spatial resolution of data. Thus it is critical to identify the three-dimensional effects, if any, of force generation due to an operational plasma actuator.

The fundamental principles of plasma actuators are continually being explored by both experimental techniques and numerical modeling. Recently, the dc corona discharges and ac dielectric barrier discharges have been investigated under a range of operating conditions. In experimental studies the V-dot probe technique on actuators in a large vacuum chamber shows that the applied potential across the electrodes is twice of the voltage drop across the plasma generated [10]. It has been identified that the electric force generation is linearly related to the surrounding air pressure [11]. Adjustment of the actuator geometry, dielectric materials, power frequency, and rms voltage show improvement in power transferred to the neutral gas flow by ion-neutral collisions [12]. For example, the electrically induced body force increases with up to the fourth power of voltage for a constant frequency [13]. The induced jet velocity thus improves with applied voltage [14,15]. Experiments show that the actuator power may be reduced by 90 percent and its durability can be improved by operating it in an unsteady manner [16]. However confusion remains about the influence of frequency. In one study the body force was found less biased by the input frequency [17], while others found it to be proportional to frequency for a constant voltage [13-15]. The influence of plasma actuators are limited by different kinds of power losses such as reactive power losses due to impedance mismatch between the power supply and the actuator, dielectric heating, plasma joule heating which need to be minimized for optimum performance [17,18].

Specific modality of discharge whether it is glow, Townsend, or streamers will help determine how the body force is transported from charge to neutral species [19]. The effect of this body force in controlling three dimensional laminar and transitional flow structures have been studied utilizing both phenomenological [20] and first-principles plasma kinetics. [21] Recent development of a loosely coupled fluid plasma formulation [22] has shown reasonable success in describing radio frequency (rf) powered electrohydrodynamic (EHD) control of NACA wing stall, laminar separation over a ramp, boundary layer transition on a flat plate, and turbulent separation over a wall-mounted hump. Unsteady flow actuation with a duty cycle seemed to perform better than

continuous operation of the rf plasma actuator. These results underscore the importance of accurately resolving the unsteady body force and understanding its transition and turbulence enhancement mechanisms for effective plasma actuation.

Numerical simulations of an asymmetrically arranged dielectric barrier discharge actuator employing multispecies hydrodynamics [14,23] and Monte Carlo particle-in-cell and direct simulation Monte Carlo methods [10] by independent research groups have found that ionization is not equal during positive and negative part of the alternating cycle producing a net force in one direction. Also, power losses due to inadequate impedance matching of the power supply to the actuator, dielectric heating, and power required to maintain the atmospheric pressure plasma have been reduced for better performance of the actuator. [17, 24]

Plasma actuator was also treated as a heat and momentum input into a small control volume [2]. Reported measurements indicate that the momentum coupling between the charged particles and the neutral particles occurs on timescales much shorter than that for the bulk fluid motion. The description of plasma-fluid interaction involves interplay between electron, ion and fluid time scales. The electron plasma frequency is $\sim 10^9$ Hz, ion plasma frequency is $\sim 10^6$ Hz and that of the fluid (speed/domain) frequency is $\sim 10^3$ Hz. As the speed increases, for example, with Mach number, the flow frequency increases and at very high speeds the ion plasma frequency may become comparable to the flow frequency. At hypersonic flows non-equilibrium chemical kinetics also affects the energy transfer mechanisms. Another mode of momentum coupling can be achieved using wall temperature injection influencing the thermal boundary layer through electrical or other means. Theoretical details of such coupling will be explored through an experiment-integrated numerical study in the near future.

An important factor in understanding the force mechanism in plasma actuators is the fundamental influence of various charged species in the working gas. PI's group has introduced a detailed numerical model of plasma actuator with eight species air chemistry with nitrogen and oxygen mixture has found effect of different charged species into the generation of electrodynamic force that controls flow of the surrounding fluid [19].

As a specific application for such model, a three-dimensional study of the discharge characteristic over a conical forebody geometry is chosen. The flight vehicle forebody vortex symmetry breaking and control of resulting yaw departure by active and passive means have been studied by many researchers [25-31]. Such study includes numerical simulation, analytical interpretation and experiments. For example, flow control using flow injection and surface heating has been investigated for asymmetric flows around circular cones by using computational solution of the unsteady, compressible full Navier-Stokes equations. [25] Various computational aspects of two-dimensional modeling have already been extensively explored [26]. Passive vortical flow control on a wing-body combination using tangential blowing has also been studied. [27] The feasibility of using forebody tangential blowing to control the roll-yaw motion of a wind-tunnel model at high angles of attack has been shown experimentally. [28] Analytical modeling for a circular cone for determining the stability of point vortices to small symmetric and asymmetric displacements were qualitatively validated against experimental results [29].

As an alternative to blowing, surface discharge plasmas may be employed to actively control or eliminate vortical asymmetry about the nose of a conical forebody at an angle of incidence. High-frequency spark discharge plasma was used to control asymmetric vortical structures on the conical forebody [30]. Results of wind tunnel experiments show that plasma actuators distributed near flow separation lines may be used for successful control or elimination of vortex asymmetry. A two-dimensional theoretical study for flow control over a conical section was reported by the PI's group using a single barrier discharge actuator and a set of dc plasma actuators [31]. Results show insufficient control of the flow on the entire length of the forebody due to a single barrier discharge actuator. Flow control on the conical forebody cross-section using several pulsed dc plasma actuators show considerable improvement for separated neutral gas flow at 17.5 deg angle of attack. In general, two-dimensional details are limited in exploring discharge constrictions and instability structures, and thus the three-dimensional analysis of force generation mechanism remains necessary.

As an extension of our two-dimensional model [3,6,31], in this effort we cast the drift diffusion discharge physics into a three-dimensional finite element framework. We apply

the formulation for modeling a set of pulsed dc plasma actuators over a three-dimensional conical forebody using plasma actuator operating in weakly ionized oxygen gas. The section II gives details of air (N_2/O_2) chemistry. The third section provides details of the computational geometry, initial and boundary conditions and numerical details. Simulation of the plasma discharge physics with applied pulsed dc potential is described in section IV. Conclusions are drawn in the final Section V.

II. AIR ELECTROCHEMISTRY

For the air chemistry we neglect the metastable species along with N^{4+} and O^{4+} due to their extremely high recombination rates. Also, the numerical complexity is further simplified by excluding nitrous oxide at this stage. The model equations governing chemistry of discharge are as follows.[32]

(1) Nitrogen model

(a) Ionization $e + N_2 \rightarrow N_2^+ + 2e$, (1a)

(b) Dissociation $e + N_2 \rightarrow 2N + e$, (1b)

(c) Dissociative recombination $e + N_2^+ \rightarrow N_2$, (1c)

(2) Oxygen model

(a) Ionization $e + O_2 \rightarrow O_2^+ + 2e$, (2a)

(b) Dissociation $e + O_2 \rightarrow 2O + e$, (2b)

(c) Dissociative attachment $e + O_2 \rightarrow O_- + O$, (2c)

(d) Recombination $O^- + O_2^+ \rightarrow O + O_2$, (2d)

(e) Dissociative recombination $O + O^- \rightarrow O_2 + e$, (2e)

The drift-diffusion form of continuity and Poisson equations for the electrons, ions and neutrals are as follows:

$$\frac{\partial n_e}{\partial t} + \nabla.(n_e \mathbf{v}_e) = k_1 n_e n_{N_2} - k_3 n_e n_{N_2^+} + (k_5 - k_7) n_e n_{O_2} + k_9 n_e n_{O_2^+}, \quad (3)$$

$$\frac{\partial n_N}{\partial t} + \nabla.(n_N \mathbf{v}_N) = 2k_2 n_e n_{N_2}. \tag{4}$$

$$\frac{\partial n_{N_2}}{\partial t} + \nabla.(n_{N_2} \mathbf{v}_{N_2}) = -k_1 n_e n_{N_2} - k_2 n_e n_{N_2} + k_3 n_e n_{N_2^+} \tag{5}$$

$$\frac{\partial n_{N_2^+}}{\partial t} + \nabla.(n_{N_2^+} \mathbf{v}_{N_2^+}) = k_1 n_e n_{N_2} - k_3 n_e n_{N_2^+} \tag{6}$$

$$\frac{\partial n_{O_2}}{\partial t} + \nabla.(n_{O_2} \mathbf{v}_{O_2}) = -(k_4 + k_5 + k_6) n_{O_2} n_e + k_7 n_{O^-} n_{O_2^+} + k_8 n_e n_{O_2^+} \tag{7}$$

$$\frac{\partial n_O}{\partial t} + \nabla.(n_O \mathbf{v}_O) = (2k_5 + k_6) n_e n_{O_2} + k_7 n_{O^-} n_{O_2^+} \tag{8}$$

$$\frac{\partial n_{O^-}}{\partial t} + \nabla.(n_{O^-} \mathbf{v}_{O^-}) = k_6 n_e n_{O_2} - k_7 n_{O^-} n_{O_2^+} \tag{9}$$

$$\frac{\partial n_{O_2^+}}{\partial t} + \nabla.(n_{O_2^+} \mathbf{v}_{O_2^+}) = k_4 n_e n_{O_2} - k_7 n_{O^-} n_{O_2^+} - k_8 n_e n_{O_2^+} \tag{10}$$

$$\nabla\cdot(\varepsilon\nabla\phi) = 4\pi e(n_e + n_{O^-} - n_{N_2^+} - n_{O_2^+}), \tag{11}$$

with momentum flux $n_\alpha \mathbf{v}_\alpha = -\mathrm{sgn}(e) n_\alpha \mu_\alpha \nabla\phi - D_\alpha \nabla n_\alpha$, and electric field $\mathbf{E} = -\nabla\phi$.

The electron temperature is calculated from $\mathbf{E} = k_B T_e/(\nabla n_e/n_e)$, which is obtained assuming an initial Boltzmann distribution, $n_e \propto \exp(e\phi/k_B T_e)$. Various rate coefficients $k_1, k_2, \ldots k_8$ related to in Eqs. (1a) through (2e) are obtained from Kossyi et al. [32] as functions of electron temperature. The secondary electron emission from the exposed surface is taken as a function of incident electron energy [33] and remains small, i.e., less than 10^{-3}. No material sputtering of the surface is considered. In Eqns. (3)-(11), n_α and $\mathbf{v}_\alpha$ are density and velocities of species α. The mobilities μ_α and diffusion rates D_α are taken from Ellis et al. [34]. Details of air chemistry simulation results considering the bulk density of the air as 1.3 kg/m^3 and an atmospheric ratio of 3.6 for nitrogen to oxygen gas molecules are described in our publication. [6] The three dimensional discharge over forebody cone is simulated using oxygen electrochemistry where the bulk density of oxygen is taken to be 0.35 kg/m^3 at atmospheric pressure.

III. NUMERICAL MODEL

Figure 2 shows schematic of a pulsed dc plasma actuator. The simulated region is 60° segment of a cone. The segment extents from z = 0.06 cm to z = 4.0 cm. The surface containing the electrodes and dielectric is given by $x = 0.16\sin(360-\alpha)$ cm to $x = 0.5\sin(360-\alpha)$ cm and $y = 0.16\cos(360-\alpha)$ cm to $y = 0.5\cos(360-\alpha)$ cm, where α varies from 0° to 60°. The domain of simulation consists of a 2 mm thick air packet coating over this curved surface. The domain size is sufficient to capture the physics of plasma dynamics.

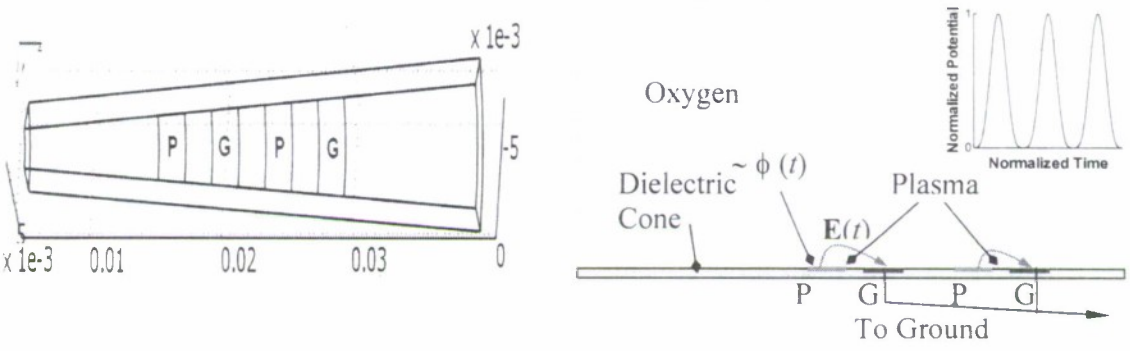

Figure 2. Schematic of three-dimensional plasma discharge on a conical forebody using pulsed dc actuators operating in oxygen gas.

We study only plasma dynamics in the present work. Present domain size is not sufficient to capture dynamics of air flow (for Navier-Stokes equations) which needs a bigger domain size. The pulsed dc plasma actuator consists of four electrodes separated by a dielectric. The powered electrodes are marked by P and grounded electrodes by G the Figure 2. The electrodes are exposed to oxygen. Thickness of each electrode is 2.0 mm along the z-direction. The powered and grounded electrodes are separated by dielectric. Thickness of dielectric separating the electrodes is 2.0 mm along the z-direction. The powered electrodes are from z = 1.6 cm to z = 1.8 cm and z = 2.4 to z = 2.6 cm. The dielectric surface between the electrodes is from z = 1.8 cm to z = 2.0 cm, z = 2.2 cm to z = 2.4 cm and z = 2.6 cm to z = 2.8 cm. The grounded electrode is from with z = 2.0 cm to z = 2.2 cm and z = 2.8 to z = 3.0 cm. We have chosen the relative dielectric constant $\varepsilon_r = 10$. The domain is filled with air of relative dielectric constant $\varepsilon_r = 1.0055$. The height of the electrodes is assumed negligible. A pulsed dc voltage of $\phi = \phi_0 \sin^4$

$(2\pi ft)$ volts is applied to the powered electrode. Such pulsed dc voltage can be produced by commercially available function generators and can be amplified. We have chosen with $\phi_0 = 1000$ volt, and $f = 5$ kHz.

Initial conditions are as follows: The all initial particle concentrations, except those of the electrons, and oxygen molecules, are taken zero. Initial atmospheric oxygen molecule density is taken as $10^{26}/m^3$, and the electron density is taken as $10^9/m^3$. Initial pulsed dc potential is zero. These initial conditions have been chosen to match with the realistic atmospheric conditions.

The boundary conditions for the Poisson's equation are as follows: The potential difference with $\phi_0 = 1000$ volt is applied to the first electrode of the pair. The other electrode of the pair is grounded. The powered electrodes are marked by **P** and grounded electrodes by **G** the Figure 2. The powered and grounded electrodes are separated by dielectric. Electric insulation condition (normal component of electric field equal to zero) is assumed at outer boundaries of the domain and at the dielectric surface.

Boundary conditions related to oxygen species continuity equations are as follows: the currents flow normal only to the rf electrode since it is an equipotential surface. Homogeneous Neumann conditions are applied to the outer edges of the domain and electric insulation is assumed at the surface of the dielectric. The normal currents at the surface of dielectric are taken zero.

The ionized oxygen gas is numerically modeled using a self-consistent three-dimensional Galerkin variational formulation based finite-element method to obtain electron, ion and neutral species densities of oxygen, and the electric potential distribution. Finite element techniques[3,4,14,18,31] are well known for their adaptability to arbitrary multidimensional geometries and accurate imposition of complicated boundary conditions. Here, the equation sets (3): (11) can be written with operator L as L (**U**) = 0 where **U** contains state variables like species number densities and potential. Multiplying with a permissible test function η and integrating over the spatially discretized domain Ω, the variational statement results in the weak form

$$WS^h = \Im_e \left(\int_{\Omega_e} [\eta L(\mathbf{U}) d\tau] \right)_e = 0 \qquad (12)$$

for a discretization h of $\Omega = \cup \Omega_e$ and $\Im_e$ is the non-overlapping sum over the elements. Application of Green-Gauss divergence theorem "weakens" the order of derivatives in (12) and yields natural homogenous Neumann boundary conditions. The surface integral thus resulting in Eqn. (12) contains the (un)known boundary fluxes wherever fixed or flux boundary conditions are enforced accurately. Thus, for example, the Galerkin form of Eqn. (11) becomes,

$$\sum_e \left(\int_{\Omega_e} \frac{d\eta}{dz} \varepsilon \frac{d\eta^T}{dz} dz \{\phi\}_e + e \int_{\Omega_e} \eta \eta^T dz \{n_e\}_e - e \int_{\Omega_e} \eta \eta^T dz \{n_{O_2^+}\}_e + e \int_{\Omega_e} \eta \eta^T dz \{n_{O^-}\}_e - \int_{\Omega_e \sim \partial\Omega_e} \eta \varepsilon \frac{d\eta^T}{dz} dz \{\phi\}_e = F_\phi \right)_e$$

where F_ϕ is the solution residual.

The Jacobian matrix $J=[\partial F/\partial \mathbf{U}]$ in the global $[J].\{\partial \mathbf{U}\} = -\{F\}$ is resolved using LU-decomposition scheme for updating change in discretized solution vector $\mathbf{U}$ at each iteration. The terminal non-linear ordinary differential equation (ODE) systems are solved using implicit Euler method for temporal evolution and N-R iterative algorithm for the non-linear matrix algebra. The convergence criterion for all variables at any iteration is set at 10^{-4}. Solution stability is ensured by appropriate selection of adaptive time marching step size (with the smallest step of one hundredth of the dielectric relaxation timescale) and the introduction of artificial diffusion. The number of degrees of freedom employed is 123816.

Independent of the physical dimension of the working domain Ω, and for general forms of the flux vectors, the semi-discretized weak statement always yields an ordinary differential equation (ODE) system that is *fully discretised* using a θ-implicit or τ-step Runge-Kutta type time integration. The terminal ODE is usually solved using a Newton-Raphson scheme for $\mathbf{U}(t)$:

$$\begin{aligned} &\mathbf{U}_{\tau+1}^{l+1} = \mathbf{U}_{\tau+1}^{l} + \Delta \mathbf{U}^l = \mathbf{U}_\tau + \sum_{p=0}^{l} \mathbf{U}^{p+1}, \text{ where} \\ &\Delta \mathbf{U}^l = -\left[\mathbf{M} + \theta \Delta t (\partial \mathbf{R} / \partial \mathbf{U}) \right]^{-1} \mathbf{R}(\mathbf{U}) \end{aligned} \qquad (13)$$

Here, a θ–implicit time marching procedure is employed. In (13), $\mathbf{M} = S_e(\mathbf{M}_e)$ is the "mass" matrix associated with element level interpolation, $\mathbf{R}$ carries the element convection, diffusion and source information. The calculation of the "Jacobian" $\partial\mathbf{R}/\partial\mathbf{U}$ and inversion of the $\mathbf{M}+\theta\Delta t(\partial\mathbf{R}/\partial\mathbf{U})$ matrix with sufficient accuracy is obviously a numerical challenge. However, unlike the traditional finite difference/volume methods, the present FE algorithm allows one to simulate the system simultaneously without requiring any sub-iteration for the Poisson solver.

In order to resolve the plasma details in three-dimensions it is crucial to resolve wall sheath region. So, we used the smallest element thickness of the order of Debye length around the powered electrode. The mesh density was proportional to the electric field intensity in all three-directions. Note in this case we are not attempting to calculate fluid flow which would require a very large domain with sub-mm scale flow mesh to be overlapped on the micron scale plasma mesh. In such case, in three-dimensions several hundreds of millions of degrees of freedoms will be solved mandating some multi level parallel coding approach and weeks of simulation time to cover all time scales. The level of computational challenge will even increase further as we include more complexity of finite rate air chemistry with large species array. We contain such challenges by solving drift-diffusion approximated plasmas incorporating only electron and four species of oxygen gas. The select set of equations from Eqn. (1): (11) are used for modeling oxygen chemistry as given in our recent paper. [35]

IV. RESULTS AND DISCUSSION

Discharge starts in the oxygen as we switch on the pulsed dc voltage. Different ion and neutral species are formed through ionization, dissociation and dissociative attachment etc. Recombination also occurs. Full chemistry of different species formation and recombination is described by Equation (2). The simulation results at the peak of the 10^{th} cycle of the pulsed dc are given in Figures 3-7.

Figure 3(a) and 3(b) show electric potential and electric field components as a function of z at $\alpha = 15°$ and 45° for a pulsed dc plasma actuator. As mentioned earlier that very first electrode from the left is powered electrode. Then there is dielectric of 2

mm thickness and then a grounded electrode. The sequence is repeated for second set of electrodes and dielectric. The variation of various components of electric field on the surface follows from applied of electric potential. Electric field is given by $\mathbf{E} = -\nabla\phi$. Since the gradient of electric field is highest at the edges the electrodes, the value of electric field is highest there. The potential does not change with z for the powered and grounded electrodes. The gradient of electric potential with respect to z is zero. The value of E_z is zero at the electrodes surfaces. The potential is not constant with respect to x or y, hence E_x and E_y are not zero at the electrode surfaces. The curvature of the electrodes with lower values of z is high; the electric field is high for these electrodes. Higher ionization occurs for these electrodes.

Figure 4 (a) shows spatial distribution of electron density for pulsed dc plasma actuator. Chemistry of electrons formation is given by set of Equation (2a). Spatial and temporal density profile of electrons is governed by continuity equations coupled with Poission equation. Electron density rises up to a level $4 \times 10^{14}/\mathrm{m}^3$. Electrons respond to electric field very fast due to low mass and high mobility. The electrons are repelled from the area of grounded electrode and are attracted towards powered electrode where they are lost. Figure 5 (a) shows slices of density of electrons at the positive peak of the pulsed dc of tenth cycle. The density decreases sharply with the increase in the distance from the surface of the electrodes and dielectric.

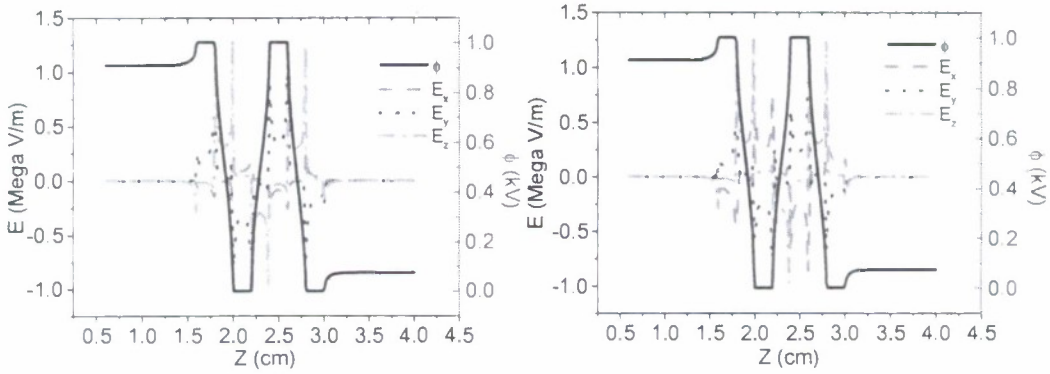

(a) $\alpha = 15^o$ (b) $\alpha = 45^o$

Figure 3. Electric potential and electric field components as a function of z.

The oxygen ions O^- are produced through dissociative attachment of oxygen molecules with electrons governed by the Eqn. (2c). Its density is governed by continuity

Eqn. (6) coupled with other equations. The density of oxygen ions O^- grows to a level of nearly $3 \times 10^{15}/m^3$. Figure 4 (b) shows density profile of negative oxygen ions O^- at positive peak of the pulsed dc of tenth cycle. The negative oxygen ions play an important role in oxygen chemistry. The oxygen ions O^- are repelled from the area of grounded electrode and are attracted towards powered electrode under the influence of pulsed dc. At the electrode oxygen ions O^- become a part of normal current. The oxygen ions O^- are much heavier than that of electrons and its mobility is low; response is slow.

The edge of the powered electrode is at z=1.8 cm. The peak of density is close to the edge of the powered electrode. Electric field is highest at the edges hence higher ionization occurs at these locations. The curvature of the electrodes at lower values of z is higher. The electric field is higher for higher curvature. This increases ionization for the electrodes with lower values of z. Figure 5 (b) shows slices of density of negative oxygen ions O^- at positive peak of the pulsed dc of tenth cycle at electrode edges. The density decreases sharply with the increase in the distance from the edge of the electrodes or dielectric.

Response of negative species to the electric field is opposite to that of positive ions. Ion mass and motilities are also different for different oxygen species and electrons, hence, their velocities are different. This gives rise to charge separation given by $n_q = n_{O_2^+} - n_e - n_{O^-}$. Figure 4 (d) shows density profile of charge separation at positive peak of the tenth cycle. It resembles that of density profiles of positive oxygen ions. The densities of charge species (such as electrons and O_2^-) are small in comparison to O_2^+ ions. The value of charge separation q is nearly equal to density of O_2^+ ions. Figure 5 (d) shows slices of density of charge separation at the edges of electrodes at positive peak of the pulsed dc of tenth cycle. The peak of charge separation is very close to the common edge of the powered electrode and dielectric. Strength and direction of electric field and charge of various species is responsible for this location of densities. Charge separation gives rise to a self-generated electric field through Poisson's Equation. The density decreases sharply with the increase in the distance from the edges of the electrodes or

dielectric. The localized hotspots near the electrodes are similar to that seen in experiments and may be signatures of DC corona instability.

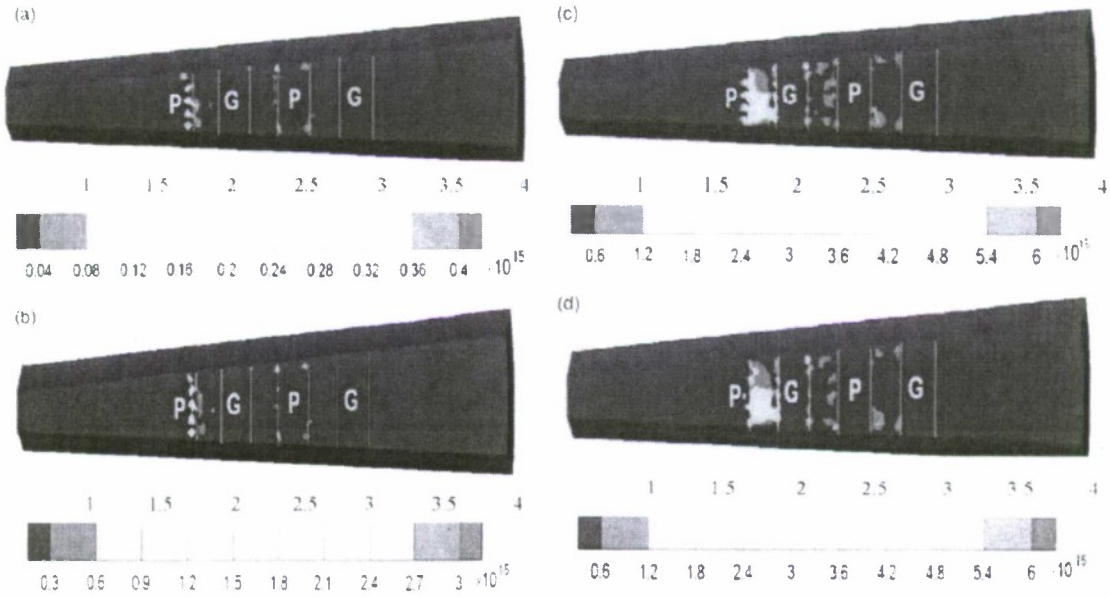

Figure 4. Surface plot of density (m^{-3}) of (a) electrons, (b) negative oxygen ions O^-, (c) positive oxygen ions O_2^+ and (d) charge separation $n_q = n_{O_2^+} - n_e - n_{O^-}$.

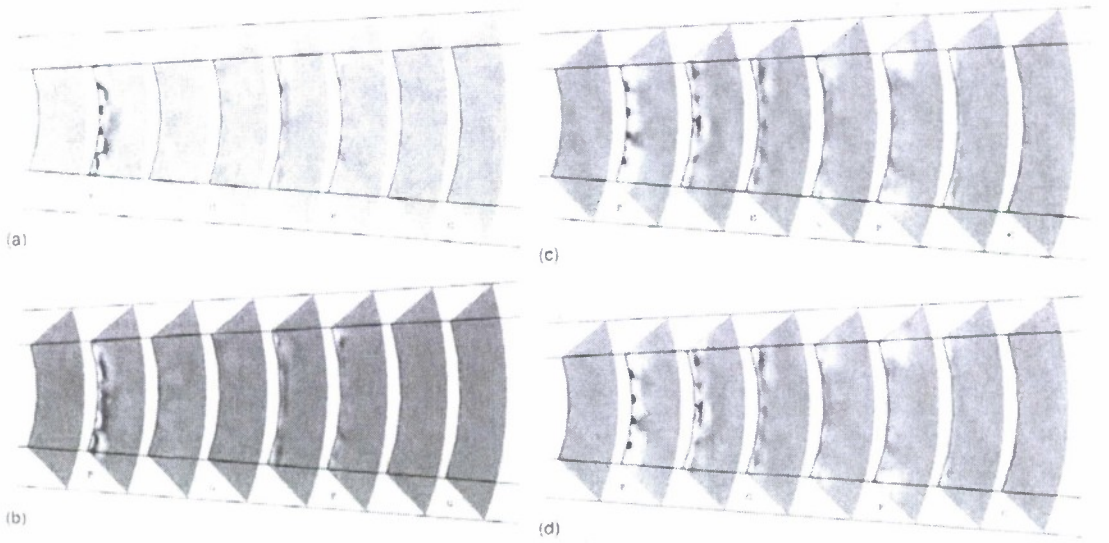

Figure 5. Slices of density (m^{-3}) of (a) electrons, (b) negative oxygen ions O^-, (c) positive oxygen ions O_2^+ and (d) charge separation $n_q = n_{O_2^+} - n_e - n_{O^-}$.

Figures 6 (a) and 6 (b) show density of various charge species at α = 15° and 45° as a function of z, respectively. These figures give us numerical estimation of variation of density of different charge species along z. Since the discharge is not uniform along the edges of the electrons, variation of charge densities in Figs. 6 (a) and 5(b) are not same.

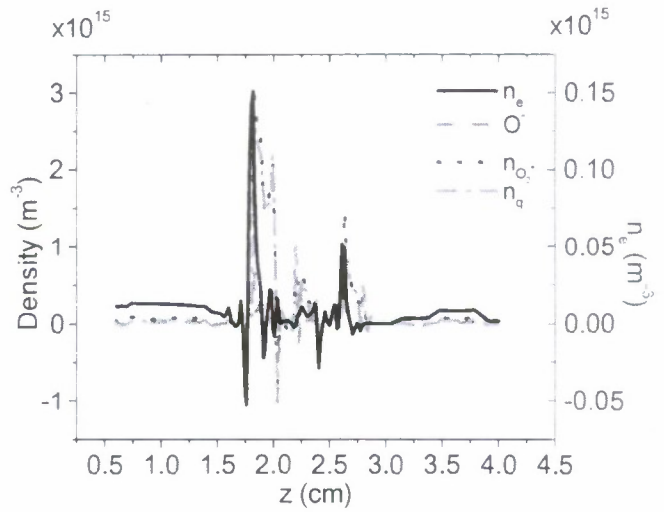

(a)

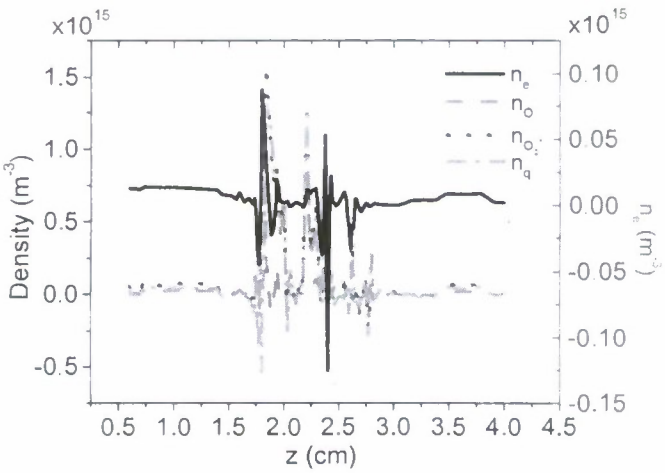

(b)

Figure 6. Density of various charge species at (a) $\alpha = 15^{o}$ and (b) $\alpha = 45^{o}$.

Figure 7 shows spatial distribution of vectors of time average of electrodynamic force $\mathbf{F} = e(n_{O_2^+} - n_e - n_{O^-})\mathbf{E}$ for pulsed dc plasma actuator. The force is strong close to the common edges of dielectric and electrodes due to high electric field and ionization. The

direction of time averaged force is in positive z-direction from powered electrode to grounded electrode (from anode to cathode). This may be useful in separation control. The solution will be sensitive to the initial conditions; we have taken only one initial condition which is close to the atmospheric condition. We have investigated the role of negative oxygen ions O_2^- in air chemistry and found that the density of negative oxygen ions O_2^- remains lower than that of positive oxygen ions O_2^+. The positive oxygen ions O_2^+ play more important role compared to O_2^-. These results have been described in our recent study [36].

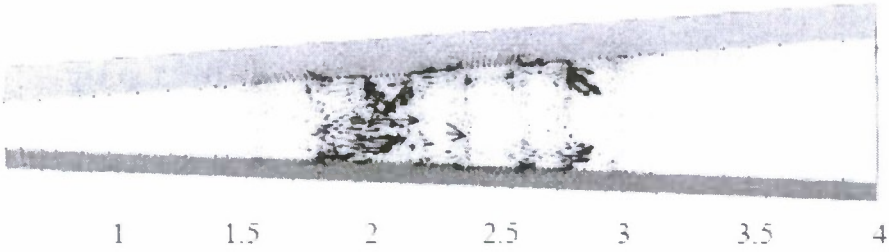

Figure 7. Vector plot of electrodynamic force $\mathbf{F} = e(n_{O_2^+} - n_e - n_{O^-})\mathbf{E}$ in perspective shows three-dimensional nature of the force distribution.

V. CONCLUSIONS

For the first time, the three-dimensional discharge about a plasma actuator operating in oxygen under pulsed dc power has been studied using a self-consistent multibody modeling of oxygen, plasma and dielectric. Chemistry of formation of different species of oxygen has been taken into account. Species with very high recombination rates and nitrous oxide have been neglected for simplicity. Continuity equations governing densities of electrons, ions and neutral species of nitrogen and oxygen are solved with Poisson's equation using a three-dimensional finite element based formulation of plasma to obtain spatial and temporal profiles of densities of species, and electric field. The electric field and ionization is the highest close to the common edges of electrodes and dielectric. Oppositely charged species move in opposite directions due to applied pulsed dc potential which gives rise to charge separation. Poisson's equation governs electric field generated due to charge separation. The density of separated charge

$n_q = (n_{O_2^+} - n_e - n_{O^-})$, and the electrodynamic force per volume $\mathbf{F} = e(n_{O_2^+} - n_e - n_{O^-})\mathbf{E}$ have been obtained. Numerical predictions show DC corona type plasma instability similar to experimental observations. The time average of the force shows mostly acceleration in the forward direction (from anode to cathode) above the actuator. This results in a moving wave of plasma over the surface in forward direction which can find application in flow control. A pulsed dc plasma actuator may be used as an alternative to the dielectric barrier discharge plasma actuator.

As a next step we would like to validate our numerical model integrating with diagnostic experiments as follows. (1) Study the barrier discharge plasma actuators in three-dimensions using first principles models; (2) Utilize the optical and spectroscopic diagnostics to improve the air chemistry models; (3) Introduce design modifications for improved actuator performance; and (4) Transition developed formulations to the RBAC/AFRL researchers in a reduced order form for incorporation into their fluid dynamic codes in a loosely coupled manner. The research will culminate into the most sophisticated modeling and the most detailed characterization of plasma based flow control devices available to-date. Gaining insight of plasma actuators will help robust, scalable actuation of transitional and turbulent flows.

Acknowledgment/Disclaimer

This work was sponsored by the Air Force Office of Scientific Research, USAF, under grant number FA9550-07-1-0131 monitored by Dr. John Schmisseur and LtCol Rhett Jefferies. The views and conclusions contained herein are those of the authors and should not be interpreted as necessarily representing the official policies or endorsements, either expressed or implied, of the Air Force Office of Scientific Research or the U.S. Government. The authors acknowledge thoughtful discussions with Drs. Datta Gaitonde and Miguel Visbal.

REFERENCES

[1] J.R. Roth, D.M. Sherman, S.R. Wilkinson, AIAA J. **38**, 7 (2000).

[2] C. L Enloe, T. E. McLaughlin, G. I. Font, and J. W. Baughn, 44th AIAA Aerospace Sciences Meeting and Exhibit, Reno, Nevada, 9 - 12 January 2006 (AIAA, Washington, D.C. 2002), Paper No. AIAA 2006-166.

[3] S.Roy and D.V.Gaitonde, 43rd AIAA Aeropsace Sciences Meeting, Reno NV, 10-13 January, 2005 (AIAA, Washington, D.C. 2002), Paper No. AIAA-2005-0160.

[4] S.Roy, K.P. Singh and D.V.Gaitonde, Appl. Phys. Lett. **88**, 121501 (2006).

[5] J. Poggie, 36th AIAA Plasmadynamics and Lasers Conference, Toronto, Ontario, Canada, 6- 9 June 2005 (AIAA, Washington, D.C. 2002), Paper No. AIAA 2005-5303.

[6] K.P. Singh and S. Roy, Modeling plasma actuators with air chemistry for effective flow control, J. App. Phys. **101**, 123308 (2007).

[7] B. Jayaraman, S. Thakur, W. Shyy, J. Heat Transfer **129**, 517 (2007).

[8] A.V. Likhanskii, M.N. Shneider, S.O. Macheret and R.B. Miles, Phys. Plasmas **14**, 073501 (2007).

[9] T.C. Corke, M.L. Post and D.M. Orlov, Prog. Aerospace Sci. **43**, 193 (2007).

[10] G. I. Font, C. L. Enloe, T.E. McLaughlin, and D. Orlov, 45th AIAA Aerospace Sciences Meeting and Exhibit Reno, Nevada 2007 (AIAA, Washington, D.C. 2002), Paper No. AIAA 2007-188.

[11] J. W. Gregory, C. L. Enloe, G. I. Font, and T. E. McLaughlin, 45th AIAA Aerospace Sciences Meeting and Exhibit Reno, Nevada 2007 (AIAA, Washington, D.C. 2002), Paper No. AIAA 2007-185.

[12] S. Pavon, J-L Dorier, Ch Hollenstein, P. Ott and P. Leyland, J. Phys. D: Appl. Phys. **40**, 1733 (2007).

[13] C. O. Porter, J. W. Baughn, T. E. McLaughlin, C. L. Enloe, and G. I. Font, 44th AIAA Aerospace Sciences Meeting and Exhibit Reno, Nevada, 9 - 12 January 2006 (AIAA, Washington, D.C. 2002), Paper No. AIAA 2006-104.

[14] K.P. Singh and S. Roy, J. Appl. Phys. **103**, 013305 (2008).

[15] M.P. Patel, T.T. Ng and S. Vasudevan, T.C. Corke, M.L. Post, T.E. McLaughlin and C.F. Suchomel, 45th AIAA Aerospace Sciences Meeting and Exhibit, Reno, NV, 8 - 11 January 2007 (AIAA, Washington, D.C. 2002), Paper No. AIAA 2007-635.

[16] T. C. Corke, B. Mertz, M. P. Patel, 44th AIAA Aerospace Sciences Meeting and Exhibit Reno, Nevada, 9 - 12 January 2006 (AIAA, Washington, D.C. 2002), Paper No. AIAA 2006-1208.

[17] J. R. Roth and X. Dai, 44th AIAA Aerospace Sciences Meeting and Exhibit, Reno, Nevada, 9 - 12 January 2006 (AIAA, Washington, D.C. 2002), Paper No. AIAA 2006-1203.

[18] K.P. Singh and S. Roy, Appl. Phys. Lett. **91**, 081504 (2007).

[19] C. Baird, C. L. Enloe, T. E. McLaughlin, and J. W. Baughn, Proceedings of the 43rd Aerospace Sciences Meeting, Reno, Nevada, 2005 (AIAA, Washington, D.C., 2002), Paper No. AIAA-2005-0565.

[20] W. Shyy, B. Jayaraman, and A. Anderson, J. Appl. Phys. 92, 6434 (2002).

[21] S. Roy, Appl. Phys. Lett. 86, 101502 (2005). K. P. Singh and S. Roy, J. Appl. Phys. 98, 083303 (2005); B. Jayaraman, S. Thakur, and W. Shyy, J. Heat Transfer 129, 517 (2007); A. V. Likhanskii, M. N. Shneider, S. O. Macheret, and R. B. Miles, Phys. Plasmas 14, 073501 (2007).

[22] D. Gaitonde, M. Visbal, and S. Roy, ASME Joint U.S.-European Fluids Engineering Summer Meeting, Miami, 2006 (AIAA, Washington, D.C., 2002), Keynote Lecture FEDSM2006-98553; M. Visbal, D. Gaitonde, and S. Roy, Proceedings of the Fluid Dynamics and Flow Control Conference, San Francisco, June 2006 (AIAA, Washington, D.C., 2002), Paper No. AIAA-2006-3230.

[23] K. P. Singh, S. Roy, and D. Gaitonde, Plasma Sources Sci. Technol. 15, 735 (2006).

[24] K.P. Singh and S. Roy, Applied Physics Letters, 91, 081504 (2007).

[25] O.A.S. Kandil, H. Hazem and C.H. Liu, AIAA Atmospheric Flight Mechanics Conference, Hilton Head Island, (SC, Washington, 1992), AIAA 1992-244.

[26] B. Jayaraman, W. Shyy, Prog. Aerospace Sci. (in press, 2007).

[27] Celik, Zcki Z. Roberts, Leonard, AIAA-1992-4430 AIAA Atmospheric Flight Mechanics Conference, Hilton Head Island, (SC, Washington,1992), Paper No. AIAA 1992-293.

[28] N. Pedreiro, S.M. Rock, Z.Z. Celik and L. Roberts, Journal of Aircraft **35**, 69 (1998).

[29] V. Shalaev, A. Fedorov, N. Malmuth, V. Zharov, and Ivan Shalaev, 41st Aerospace Sciences Meeting and Exhibit, Reno, Nevada, 6-9 January 2003, (AIAA, Washington, D.C. 2002), Paper No. AIAA 2003-34.

[30] A. A. Maslov, B. Y. Zanin, A. A. Sidorenko, B. V. Postnikov, V. P. Fomichev, A. D. Budovsky, and N. Malmuth, 43rd AIAA Aerospace Sciences Meeting and Exhibit, Reno, Nevada, 2005, (AIAA, Washington, D.C. 2002), Paper No. AIAA-2005-400.

[31] K.P. Singh and S. Roy, J. App. Phys. **101**, 093301 (2007).

[32] I. A. Kossyi, A. Yu Kostinsky, A.A. Matveyev and V.P. Silakov, Plasma Sources Sci. Techol. **1**, 207 (1992).

[33] S. Roy and B.P. Pandey, Phys. Plasmas, **9**, 4052 (2002).

[34] H.W. Ellis, R. Y. Pai, E. W. McDaniel, E. A. Mason, and L. A. Viehland, At. Data Nucl. Data Tables, **17**, 177 (1976).

[35] K.P. Singh and S. Roy, Journal of Applied Physics, 103 (10) 103303 (2008).

[36] K.P. Singh and S. Roy, Applied Physics Letters, 92 (11) 111502 (2008).

Personnel Supported During Duration of Grant

Richard Anderson	Graduate Student, University of Florida, Gainesville
Chin-Cheng Wang	Graduate Student, University of Florida, Gainesville
Kunwar P. Singh	Post-doctoral Associate, University of Florida, Gainesville
Subrata Roy	Associate Professor, University of Florida, Gainesville

Relevant Publications (2007-2008)

Wang, C.C. and S. Roy, "Electrodynamic enhancement of film cooling of turbine blades," J. Appl, Phys. 104 (7) Scheduled for Oct 2008.

Roy, S. and C.C. Wang, 2008, "Plasma actuated heat transfer," Applied Physics Letters 92, 231501.

Singh K.P. and S. Roy, 2008, "Force generation due to three dimensional plasma discharge on a conical forebody using pulsed dc actuators," Journal of Applied Physics, 103 (10) 103303.

Singh K.P. and S. Roy, 2008, "Physics of plasma actuator operating in atmospheric air," Applied Physics Letters, 92 (11) 111502.

Singh K.P. and S. Roy, 2008, "Force approximation for a plasma actuator operating in atmospheric air," Journal of Applied Physics, 103 (1) 013305.

Singh K.P. and S. Roy, 2008, "Flow control on a three dimensional forebody using pulsed dc plasma actuator operating in air," AIAA-2008-1102, 46th AIAA Aerospace Sciences Meeting and Exhibit.

Singh K.P. and S. Roy, 2007, "Impedance matching for an asymmetric dielectric barrier plasma actuators," Applied Physics Letters, 91 (8) 081504.

Singh K.P. and S. Roy, 2007, "Modeling plasma actuators with air chemistry for effective flow control," Journal of Applied Physics, 101 (12) 123308.

Singh K.P. and S. Roy, 2007, "Vortical flow control on a conical forebody cross-section using an array of pulsed dc actuators," Journal of Applied Physics, 101 (9) 093301.

Roy, S., K.P. Singh, and D. Gaitonde, 2007, "Air plasma actuators for effective flow control," AIAA-2007-184, 45th Aerospace Sciences Meetings, Reno, NV.